DOI: https://doi.org/10.4038/jmtr.v10i1.77

JOURNAL OF MULTIDISCIPLINARY & TRANSLATIONAL RESEARCH

Journal of Multidisciplinary and Translational Research (JMTR)

journal homepage: https://journals.kln.ac.lk/jmtr/

Enhanced adsorption of MCPA pesticide using a novel sand/graphene oxide composite

Ruwan T. Perera[1,3]*, Rajith. A. Perera[2,3], N.M.N. Ruwanthi[1], A.V.A.P. Vitharama[1], Amila T. Kannangara[2], Janitha A. Liyanage[2,3], and A.R. Kumarasinghe[4]

[1]*Department of Indigenous Medical Resources, Gampaha Wickramarachchi University of Indigenous Medicine, Sri Lanka*
[2]*Department of Chemistry, University of Kelaniya, Sri Lanka*
[3]*CKDu Information and Research Centre, University of Kelaniya, Sri Lanka*
[4]*Department of Physics, University of Sri Jayewardenepura, Sri Lanka*

Abstract

Developing graphene-based composites for mitigating water pollutants is crucial, as current composites often have limitations, including their specific adsorption behavior towards only one type of contaminant. Additionally, these existing composites are associated with high costs, challenging recovery processes, and potential toxicity to both the environment and human health. Multiple coated sand/graphene oxide composites (M-GO/S) present a promising solution to these challenges. In this study, we focused on investigating the adsorptive removal of the pesticide 2-methyl-4-chlorophenoxyacetic acid (MCPA) using M-GO/S composites. Additionally, we aimed to elucidate the underlying adsorption mechanism and develop an HPLC method for analyzing MCPA. The retention time for MCPA was determined to be 1.538 minutes. The optimal parameters for MCPA adsorption onto M-GO/S were established as a 75 mg/L MCPA concentration, a dosage of 0.05 g, and a contact period of 105 minutes at neutral pH. The isotherm studies indicate that it is challenging to distinctly classify the adsorption process using the Langmuir and Freundlich models, as they show similar R^2 values. This may be attributed to the likely occurrence of multilayered attachment of MCPA following an initial monolayer adsorption. The adsorption intensity (n) value of 0.625 further suggests that complex interactions are involved in MCPA adsorption, likely due to the surface complexity of the M-GO/S composite. Apart from that, the kinetics studies revealed that the rate-controlling step involves chemical adsorption between the surface of M-GO/S and MCPA. Chemical interactions arise through hydrogen bonding and critical interactions between the hydroxyl groups on M-GO/S and the aromatic rings of MCPA. M-GO/S is a promising candidate for the adsorptive removal of negatively charged pesticide molecules like MCPA. It outperforms activated carbon and sand in effectiveness, and it is more advantageous than graphene oxide due to its simple recovery process.

Keywords: Adsorption, Graphene oxide, MCPA, Sand, Pesticide

Article info

Article history:
Received 20th January 2025
Received in revised form 22nd February 2025
Accepted 30th February 2025
Available online 1th June 2025

ISSN (E-Copy): ISSN 3051-5262
ISSN (Hard copy): ISSN 3051-5602
Doi:
ORCID iD: https://orcid.org/0000-0001-5695-6579

*Corresponding author:
E-mail address: wprtp@gwu.ac.lk (Ruwan T. Perera)

Introduction

Toxic organic pollutants, such as aromatic compounds, pesticides, and dyes, significantly contribute to health risks and environmental damage (Uddin et al., 2009). The extensive use of pesticides in water sources presents a critical concern. Even in minimal concentrations, pesticides can cause severe health issues, including neurological disorders, liver damage, skin and eye conditions, hormonal disruptions, congenital disabilities, and cancer (Li et al., 2020). Extensive research has focused on using graphene-based composites to mitigate pesticide molecules in water, leveraging graphene's unique properties. These properties include high surface area, flexibility in functionalization, and strong adsorption capabilities (Lazarević-Pašti et al., 2018; Paramasivan et al., 2019).

Abo El-Maali. (2018) et al evaluated three nanoparticle materials, including graphene, for their efficacy in removing organochlorine, organofluorine pesticides, and various bacteria from water. Their findings indicated that graphene was the most effective in pesticide removal, highlighting the potential of graphene composites in water remediation (Abo El-Maali et al., 2018). Suo et al. (2018) developed an activated carbon derived from cellulose/graphene oxide composites material for the removal of organophosphorus pesticides, demonstrating a high adsorption capacity that surpassed other sorbents and effectively removed pesticides from water (Suo et al., 2018).

Mandeep, Gulati, and Kakkar (2020) reviewed the use of graphene-based materials for eliminating toxic organic pollutants, including pesticides, from water. Their review encompassed both experimental and theoretical studies, addressing the challenges and future perspectives of employing graphene-based materials for water remediation (Mandeep et al., 2020a). Apart from that, the expansive surface area of GO nanosheets provides numerous adsorption sites, while their oxy-compound groups enhance chemical reactivity, making them highly effective at capturing and neutralizing pollutants (Chu et al., 2020). Chu et al. (2020) demonstrated the use of size-tunable GO as a mimic for horseradish peroxidase in the colorimetric detection of organophosphorus pesticides at nanomolar levels, showcasing high sensitivity and stability, which suggests significant potential for public health applications (Chu et al., 2020). In 2021, Nasiri and colleagues developed magnetic graphene oxide coated with polyvinyl alcohol (PVA@MGO) to act as an adsorbent for removing organophosphorus pesticides from both apple juice and environmental water samples (Nasiri et al., 2021). This study highlighted the efficiency of the composite in preconcentration and detection of organophosphorus pesticides , indicating its suitability for high-throughput analysis. Among commonly applied pesticides, MCPA is an irritant to the skin and eyes. It is highly toxic and hazardous, posing significant risks even at very low concentrations, and can have harmful effects on both animals and the environment. Environmental levels of MCPA are generally detected in the μg/L range, with typical concentrations found in surface and groundwater rarely exceeding these levels. This indicates that MCPA is usually present in low concentrations in natural water bodies due to its agricultural use (Garrido et al., 2012).

However, natural water contaminated by pollutants often contains numerous contaminants, not only pesticides, but also toxic metals and other harmful organic molecules. Therefore, it is crucial to achieve the simultaneous removal of these contaminants from water. By coating sand with graphite oxide five times, the resulting "super sand" (M-GO/S) incorporates additional functional groups, enhancing its properties with those of graphite oxide. Our previous studies proved that the modified sand (M-GO/S) achieves over 70% fluoride removal and 87% turbidity reduction, making it a viable agent for water treatment (Kumarasinghe et al., 2021a). The investigation also focused on the removal of calcium ions from graphene oxide-coated sand granules. The M-GO/S proved to be the most efficient in removing calcium ions from hard water (Perera, 2023).

Sand serves as a cost-effective, stable, and practical support for graphene oxide (GO), significantly enhancing the overall performance of the material. Incorporating sand with GO in a composite increases adsorption by expanding the surface area and preventing GO aggregation, thereby maintaining efficiency. Sand also improves the stability of GO and handling, making it easier to use and recover (Yuqing et al., 2024). Additionally, we successfully developed M-GO/S by coating GO onto the surface of sand through a thermal annealing process, marking the first time this has been achieved without the use of a binding agent. This combination reduces costs, making large-scale applications more affordable. Additionally, sand improves the settling properties, simplifying post-treatment separation from water. Thus, the physical qualities of sand enhance the performance and utility of GO in water treatment applications (Jia et al., 2022; Wang et al., 2016).

According to our previous studies, microscopic and spectroscopic characterization of M-GO/S revealed the presence of a non-uniform GO layer on the sand and the integration of oxygenated functional groups into the composite structure. The focus of this study is to investigate the efficiency of MCPA adsorption on a graphene-based composite (M-GO/S) and to understand the mechanism of the adsorption process. Additionally, a novel HPLC method was developed to analyze MCPA in contaminated water at ppm range.

Material and Method

Materials

Natural vein graphite (NVG) with an ash content exceeding 99.95% was sourced from Sri Lanka (coordinates: 7° 06' 58.49'' N, 80° 18' 34.41'' E), (Chen et al., 2013). Sand was collected from the Mahaweli River in Sri Lanka (coordinates: 8° 27' 59.99" N, 81° 13' 60.00" E). Analytical grade 2-methyl-4-chlorophenoxyacetic acid (MCPA), sulfuric acid, hydrochloric acid, hydrogen peroxide, potassium permanganate, sodium hydroxide, sulfuric acid, and activated carbon were obtained from Sigma-Aldrich (USA), BDH (UK), Daejung Chemicals & Co. Ltd. (Korea), Research-Lab Fine Chem Industries (Pvt) Ltd., Merck Life Science Private Limited, and HiMedia Laboratories Pvt. Ltd., Mumbai, India. Ultrapure water was used throughout the experiments.

Synthesis of GO - sand composites

The powdered NVG flakes were sieved through an ASTM No. 40 screen before being used to synthesize graphite oxide (GO) via a modified Hummers method. The synthesis of both GO and M-GO/S followed the procedures detailed in the referenced method (Kumarasinghe et al., 2021a).

Development of the HPLC method

The High-Performance Liquid Chromatography (HPLC) protocol for quantifying MCPA adsorption was developed using a solvent mixture of acetonitrile and distilled water in a 50:50 ratio. This combination was selected for its effectiveness in eluting and separating MCPA molecules. A precise flow rate of 1.5 µL/min was maintained to ensure consistent elution, allowing for accurate measurement of MCPA levels. Additionally, a detection wavelength of 275 nm was selected to match the absorbance characteristics of MCPA, enhancing the sensitivity and specificity of the method. The analysis was conducted using an Agilent 1260 Infinity II HPLC instrument.

Optimization

The use of higher concentrations, such as in the mg/L range, in this study is justified by the need to simulate worst-case scenarios or to understand the adsorption capacity and efficiency of the developed materials under conditions of elevated contamination, which might occur due to spills or high-intensity agricultural runoff. These higher concentrations allow for a comprehensive evaluation of the performance of the adsorbent across a broader range of potential environmental conditions. All optimization studies were conducted in triplicate.

Concentration Optimization

The experimental setup involved meticulously preparing samples at various MCPA concentrations: 50, 75, 100, 125, and 150 mg/L. These MCPA solutions were systematically dispensed into 100 mL Erlenmeyer flasks, with each solution precisely measured to a volume of 25 mL. This approach ensured a comprehensive analysis across a diverse range of concentrations, providing a nuanced understanding of the adsorption behavior at varying MCPA concentrations. Each step was executed with precision to maintain the integrity and accuracy of the experimental setup.

The adsorption process commenced with the careful addition of 0.1g of M-GO/S into each flask containing the MCPA solutions. The flasks were then placed on an open-air shaker and subjected to continuous agitation for two hours at a rotational speed of 120 rpm. After agitation, the liquid phases were filtered through a 0.45 µm nylon filter membrane. The filtrates were then analyzed using High-Performance Liquid Chromatography (HPLC) to quantify any residual MCPA. This systematic procedure ensured a controlled and uniform adsorption process, laying the groundwork for accurate analysis and reliable results.

Dosage Optimization

MCPA solution (10 mL) at a concentration of 75 mg/L was precisely distributed into 100 mL Erlenmeyer flasks. Each of these flasks contained a certain amount of the chosen adsorbent material (0.01, 0.02, 0.03, 0.04, 0.05, 0.075, 0.1, 0.125, 0.150, 0.175 g). The loaded flasks were placed within an open-air shaker that was programmed to rotate at a controlled rate of 120 rpm. After the two hours adsorption period, the liquid phase with adsorbed MCPA species was separated from the solid phase using a 0.45 µm nylon filter membrane. The filtrates were then tested for residual MCPA.

Contact time Optimization

The study investigated the optimal contact time for the adsorption of MCPA in a 100 mL Erlenmeyer flask containing 0.05 g of M-GO/S and a 75 mg/L MCPA concentration. The solution's pH was kept neutral, and it was continuously agitated for 3 hours. Samples were collected at specific intervals (every 15 minutes), and the liquid phase was filtered and separated for further analysis. HPLC was employed to analyze the residual MCPA concentration as part of kinetic study.

Adsorption isotherm

Adsorption isotherm studies were conducted on M-GO/S to evaluate their adsorption behavior across different concentrations of MCPA (50, 75, 100, 125, and 150 mg/L). The adsorption process was initiated with continuous agitation in a shaker for 105 minutes, followed by the separation of the liquid phase from the solid phase using 0.45 µm nylon membrane filters. The resulting adsorbates were analyzed for residual MCPA using HPLC. Langmuir constants, and Freundlich constants were calculated based on the following equations.

The linear form of the Langmuir equation can be written as: (Faysal Hossain et al., 2020),
Where,

Equation 1

$$\frac{C_e}{q_e} = \frac{1}{K_L.Q_{max}} + \frac{C_e}{Q_{max}}$$

q_e = Equilibrium adsorption capacity (mg/g)
Q_{max} = Maximum adsorption capacity (mg/g)
C_e = Equilibrium aqueous concentration of adsorbate (mg/L)
K_L = Constant related to the energy of adsorption (L/mg)

Hence a plot of C_e/q_e vs C_e gives $1/Q_{max}$ as the slope and $1/K_LQ_{max}$ as the intercept.
The linear form of the Freundlich equation can be represented as (Faysal Hossain et al., 2020),

Equation 2

$$logq_e = logK_F + \frac{1}{n}logC_e$$

Where, K_F and n: Freundlich constants which correspond to adsorption capacity and adsorption intensity.

C_e: Equilibrium concentration in solution, Q_e: Adsorbed capacity

Adsorption kinetics

The adsorption kinetics of MCPA on M-GO/S were investigated using a batch reactor setup with a volume of 100 mL. To conduct this study, a solution containing 100 mg/L of MCPA was prepared in a 100 mL water-jacketed batch reactor, which also included 0.05 g of M-GO/S. The reactor was continuously purged with N_2 gas to maintain an inert environment. The system was then subjected to agitation at 60 rpm on a shaker, kept at room temperature (28°C) for a duration of 120 minutes. At every 20-minute interval, 6.0 mL samples were extracted, passed through a 0.45 µm nylon filter membrane for filtration, and analyzed for remaining MCPA concentrations using HPLC. Throughout these procedures, the solution's pH was kept stable at 7.00. The adsorbed MCPA amount, and the adsorption efficiency percentage were determined from the filtrate analyses. Based on the following equations, graphs for the pseudo-first-order and pseudo-second-order models were plotted.

The pseudo-first-order equations can be written as (Imamoglu & Tekir, 2008)

Equation 3

$$\log(q_e - q_t) = log q_e - \frac{K_{1,ads}t}{2.303}$$

Where, q_t and q_e are the numbers of MCPA molecules adsorbed per mass of sorbent (mg/g) at any time and at equilibrium, respectively, and K_1, ads is the rate constant of first-order adsorption (min^{-1}). The straight-line plot of log (qe − qt) vs t gives log (qe) as slope and intercept equal to K1, ads/2.303.

The pseudo-second-order equations can be written as (Imamoglu & Tekir, 2008),

Equation 4

$$\frac{t}{q_t} = \frac{1}{K_{2,ads}q_e^2} + \frac{t}{q_e}$$

Where, q_t and q_e are the numbers of MCPA molecules adsorbed per mass of sorbent (mg/g) at any time and at equilibrium, respectively, and K2, ads is the rate constant of second-order adsorption (g (mg min) −1).

The straight-line plot of t/ q_t vs t gives 1/q_e as slope and 1/ (K_2, ads qe2) as the intercept.

Adsorption Mechanism of MCPA on the Surface of M-GO/S

Fourier Transform Infrared (FTIR) Spectroscopy spectra, ranging from 500 cm^{-1} to 4000 cm^{-1}, were recorded for M-GO/S both before and after the MCPA adsorption process. These spectral measurements were performed using a Thermo Scientific spectrometer, with pure KBr serving as background material. To facilitate the measurements, all samples were thoroughly mixed with oven-dried KBr and then compressed into transparent tablets, ensuring a standardized and consistent methodology.

MCPA Adsorption Using Commercially Available Activated Carbon and Sand

The research aimed to evaluate the adsorption potential of activated carbon and standard filtered sand. A precise amount of 0.05 g of each material was placed in separate 100 mL Erlenmeyer flasks. To each flask, 10 mL of a 75 mg/L MCPA solution was added, with the pH carefully maintained at neutral to ensure consistent conditions across all experiments. The flasks were then placed on a shaker and agitated at a constant speed of 120 rpm to promote optimal interaction between the MCPA and the adsorbents. All experiments were conducted at ambient temperature, and the MCPA concentration was subsequently analyzed using HPLC. All experimental studies were conducted in triplicate.

Results and Discussion

Development of the HPLC method

The detailed analysis of MCPA adsorption was performed using High-Performance Liquid Chromatography (HPLC). The mobile phase, consisting of a 50:50 mixture of acetonitrile and distilled water, was chosen to maximize the elution of the MCPA molecules. The flow rate was set at 1.5 µL/min to ensure steady elution, and the wavelength was set at 275 nm based on the absorbance characteristics of MCPA. This HPLC setup enabled a thorough investigation into MCPA adsorption, emphasizing analytical accuracy and consistency.

In this study, the retention time of MCPA was recorded at 1.538 minutes (Figure 1), reflecting the time required for MCPA to pass through the chromatographic column for detection. Determining the retention time is crucial for identifying and quantifying MCPA in samples, providing essential data on its chromatographic behavior. This successful determination validates the HPLC methodology, confirming its effectiveness and precision in analyzing MCPA.

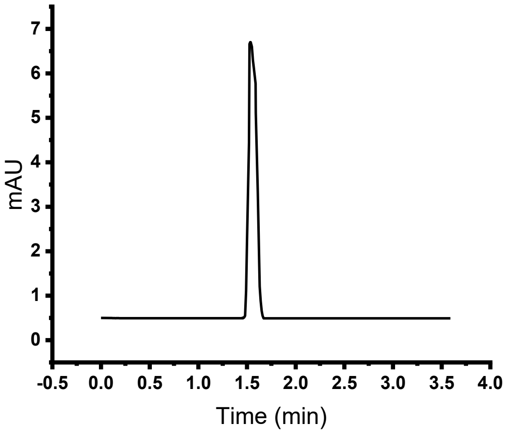

Figure 1. Chromatogram of High-Performance Liquid Chromatography (HPLC) of MCPA

Optimized studies for MCPA adsorption to Super sand

The concentration optimization, illustrated in Figure 2 (a), was carried out with a consistent application of 0.1 g of the selected adsorbent at neutral pH. Optimal adsorption of MCPA was observed at a concentration of 75 mg/L. A unique bell-shaped curve emerged during this phase, indicating that adsorption efficiency decreased when concentration levels deviated from 75 mg/L. The detailed study on MCPA removal efficiency, depicted in Figure 2 (b), examined the influence of adsorbate dosage under neutral pH conditions with an initial MCPA concentration of 75 ppm. The results revealed a positive correlation between the dosage amount and removal efficiency, with the maximum efficiency observed at an adsorbate dosage of 0.075 g. As the contact time was systematically extended, a steady increase in MCPA adsorption was observed, (Figure 2(c)). This increase continued until reaching equilibrium at 120 minutes, beyond which the adsorption leveled off.

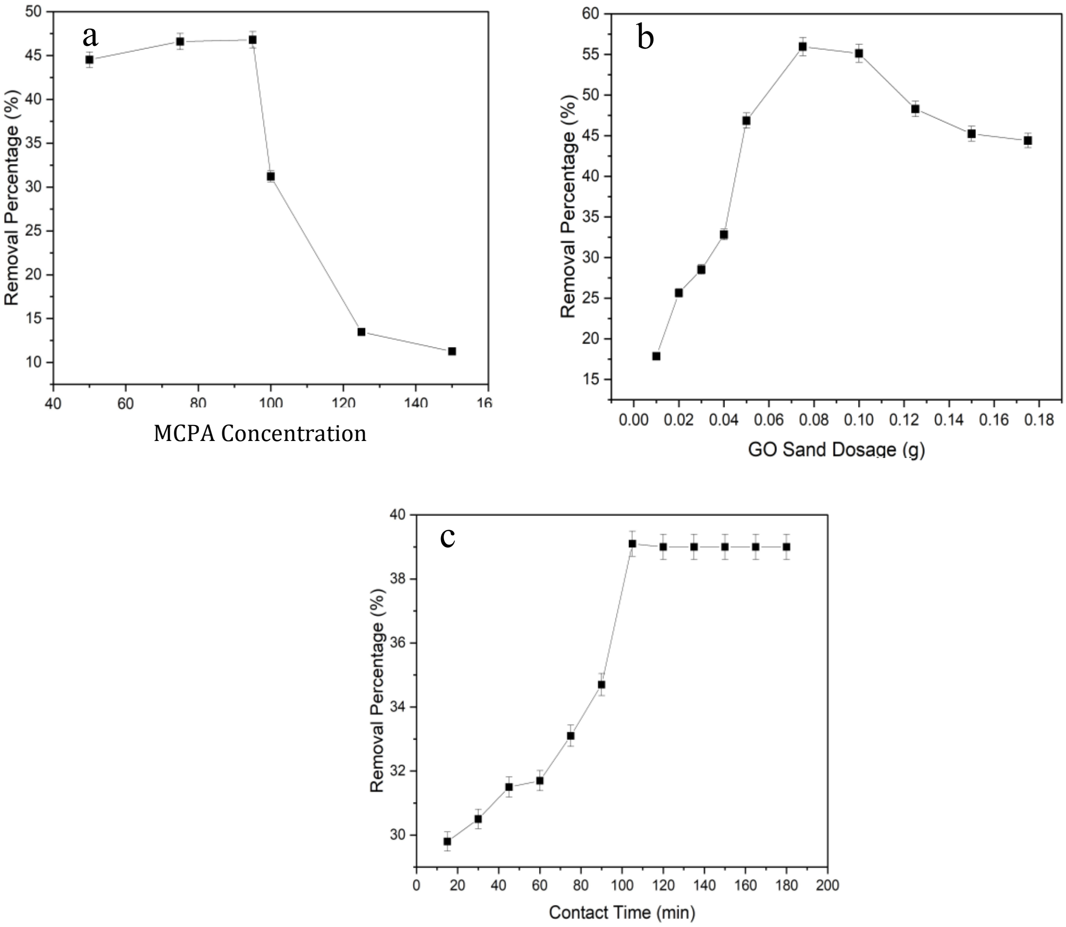

Figure 2. The graphs of MCPA adsorption percentage (%) vs. (a) MCPA concentration (mg/L), (b) M-GO/S dosage (g), (c) Time (min).

Adsorption Isotherm

Table 1: Isotherm parameters for adsorption of MCPA onto M/GO-S.

	Langmuir Constants	
Q_{max} (mg/g)	K_L (L/mg)	R^2
0. 078	0.00363834	0.995
	Freundlich Constants	
K_F (adsorption capacity)	n (adsorption intensity)	R^2
5.63378×10-5	0.625	0.9987

To identify the most suitable model for the adsorption process, correlation coefficient values (R^2) were considered (Figure 3). The results indicated that the Freundlich adsorption isotherm was the best fit for describing the adsorption of MCPA onto the super sand surface, with an R^2 value of 0.9987. The Langmuir adsorption isotherm also showed a high R^2 value of 0.995, suggesting that both models fit well due to the adsorption mechanism involving both physisorption and chemisorption (Jeppu & Clement, 2012). On the other hand, n, which delves into adsorption intensity, provides valuable insights into the strength and nature of the adsorption process. The n value, derived from the experimental isotherm study and documented in Table 1, reordered as 0.625. This value indicates a deviation from linearity in the MCPA adsorption process, suggesting a more complex interaction between the adsorbate and the adsorbent material. The fact that n is less than 1 implies that the adsorption of MCPA onto the material involves more than a straightforward, linear process, hinting at a complex chemical reaction rather than just a simple physical attachment (Imamoglu & Tekir, 2008).

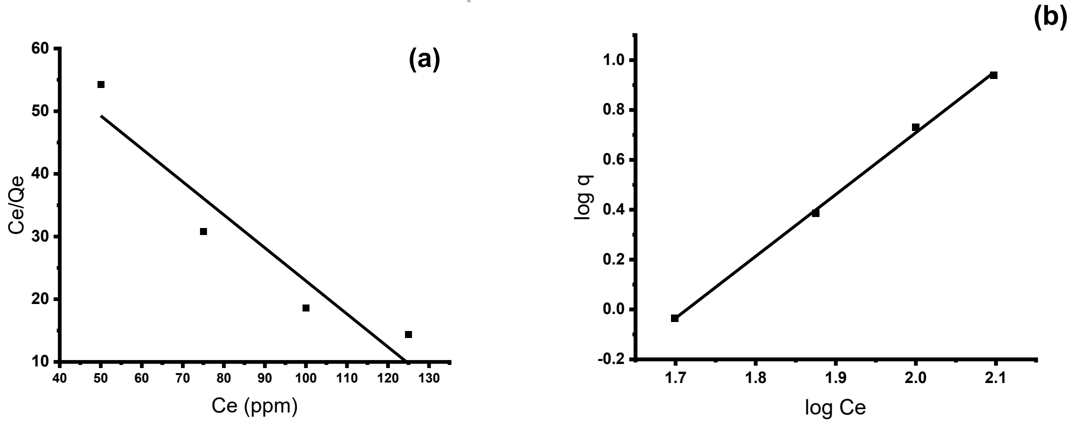

Figure 3. (a). Langmuir adsorption isotherm of MCPA sorption (adsorbent dose = 0.05g, contact time = 105 Minutes, initial concentration = 50 –150 mg L-1, agitation speed = 120 rpm, T = 25±2 °C) (R2 = 0.995), (b). Freundlich adsorption isotherm of MCPA sorption (adsorbent dose = 0.05g, contact time = 105 Minutes, initial concentration = 50 –125 mg L-1, agitation speed = 120 rpm, T = 25±2 °C) (R2 = 0.9987)

Adsorption Kinetics

The correlation coefficient for the pseudo-first-order kinetic model was 0.909, while the second-order model had a significantly higher coefficient of 0.975 (Figures 4 a, 4b), indicating a better fit. This close match to a perfect fit (1.0) emphasized the superior association of data points with the second-order model.

The study concluded that the second-order adsorption model best described the complex MCPA adsorption process onto the specially made sand gravels, providing an accurate depiction of the kinetics. This model suggested that the rate-controlling step likely involved chemical adsorption, where electrons are shared or transferred between the adsorbent and MCPA (Lian et al., 2020; Wu et al., 2009).

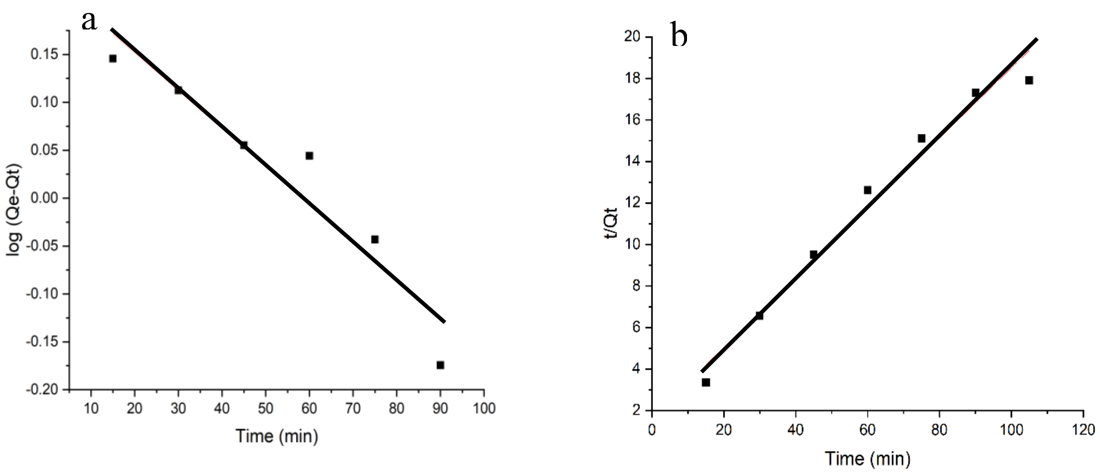

Figure 4. Adsorption kinetics of MCPA **on Surface of M-GO/S** a) Pseudo first order kinetics b) Pseudo second order kinetics.

Adsorption Mechanism of MCPA on Surface of M-GO/S

Fourier Transform Infrared (FTIR) spectroscopy was employed to characterize the interactions between MCPA and the M-GO/S surface. When considering M-GO/S, it exhibited several peaks at approximately 3770 cm^{-1}, 1742 cm^{-1}, 1551 cm^{-1}, 1091 cm^{-1}, 840 cm^{-1}, and 605 cm^{-1}. The 3770 cm^{-1} peak appears broad, suggesting the presence of –OH groups. The relative intensities of the terminal –OH bands of sand, specifically at 3650 cm^{-1} and 3720 cm^{-1}, are retained. Additionally, there is a noticeable increase in intensity at 1080 cm^{-1}, attributed to –Si–O–H bending vibrations, upon the interaction of GO with the surface sites of the sand. The bands observed at 850 cm^{-1} and 810 cm^{-1} correspond to Si–O and Si–O–Si bending vibrations, respectively (Figure 5) (Mandeep et al., 2020b).

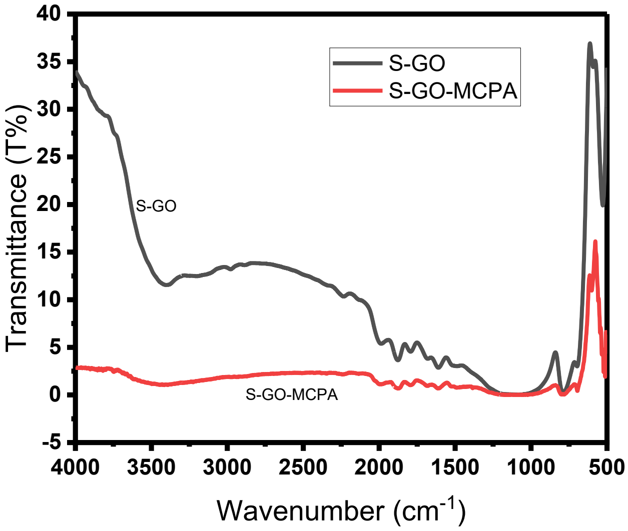

Figure 5. Overlapped FT-IR spectrum of M-GO/S before (S-GO) and after MCPA adsorption (S-GO-MCPA) under the optimum conditions.

In the spectrum, there are several peak patterns ranging from 1091 to 605 cm $^{-1}$, displaying a transition from distinct to broad characteristics. These patterns can be attributed to vibrational coupling resulting from various modes, including ≡SiOH and ≡SiO-G-O, further confirming a significant interaction between the sand and GO (Kumarasinghe et al., 2021b).

The diminished transmission in the OH region of the FT-IR spectrum suggests that the OH groups are involved in interactions with MCPA, leading to increased IR absorption at those wavelengths. This interaction can alter the vibrational energy of the OH bonds, causing the observed reduction in transmittance. However, this observation should be interpreted with caution, as other factors, such as the presence of additional absorbing species, could also contribute to the reduced transmittance (Figure 5). Within the context of MCPA, assuming its anionic state upon dissolution in water, a strong interaction occurs between the surface hydrogens of the hydroxyl groups on the adsorbent surface and the oxygen atom of the MCPA anion. This interaction, defined as "dipole-dipole interactions (hydrogen bonding)" and this chemical scenario, existing MCPA in its anionic state, bears a predominantly negative charge (Moral et al., 2012).

The term "surface hydrogens of the hydroxyl groups" specifically denotes the hydrogen atoms situated within the hydroxyl (-OH) functional groups on the surface of the adsorbent (Mahdavi-Shakib et al., 2021).These hydrogen atoms function as "H-donors," exhibiting the capability to participate in hydrogen bond formation by donating a hydrogen atom (H+). Conversely, the reference to "appropriate atoms (i.e., oxygen; H-acceptors) of MCPA" underscores the pivotal role played by the oxygen atom within the MCPA anion.

In this intricate molecular interplay, the oxygen atom serves as an "H-acceptor," actively engaging in the acceptance of a hydrogen atom during the hydrogen bond formation process. This interaction shows how surface hydrogen atoms and oxygen atoms work together in a specific and complex way through hydrogen bonding in this chemical situation (Lian et al., 2021).

Yoshida hydrogen bonding is an important interaction between M-GO/S hydroxyl groups and MCPA aromatic rings. This hydrogen bonding, together with dipole-dipole interactions, is critical for the adsorption of MCPA onto the adsorbent. These complicated molecular interactions describe the chemical interaction between MCPA and the adsorbent, furthering our understanding of the efficiency of the adsorption process and selectivity while also adding complexity to adsorption dynamics (Osawa et al., 1967).

In 1969, Mattson and colleagues proposed n-π interactions, which add to the complexity of hydrogen bonding. This interaction adds dimension to the molecular conversation that occurs throughout the adsorption process between the adsorbents surface and the MCPA pesticide (El-Shamy et al., 2023). The addition of n-π interactions increases the complex structure of forces at work, adding to the varied aspects of the adsorption mechanism (Zhu et al., 2005). The carbonyl oxygens in the adsorbent form n-π interactions with the aromatic rings in MCPA , where the carbonyl oxygens donate electrons to the aromatic rings. FT-IR spectra show shifts and decreased intensity in C=O and C-O peaks following MCPA adsorption, demonstrating these interactions (Hasanuddin et al., 2020).

Comparison of MCPA adsorption with reference material (Commercially available activated carbon, and sand)

M-GO/S showed better MCPA adsorption efficiency 56.13% (±0.32) than activated carbon (20.90 ±1.32%), and sand (13.20 ±2.32 %) (Figure 6). This better performance is attributed to M-GO/S's surface characteristics, resulting in it being a more effective adsorbent to eliminate MCPA from contaminated water. The M-GO/S composite is designed to be environmentally friendly, as it is composed of graphene oxide (GO) and sand, both of which are non-toxic and safe for use in water treatment. Additionally, the easy recovery process of the material after purification further minimizes environmental impact (Gao et al., 2011).

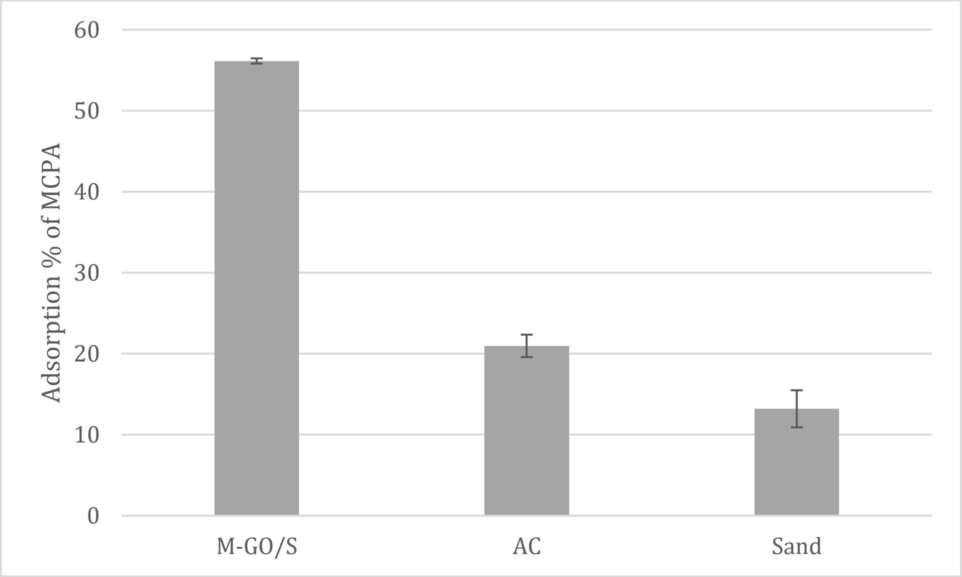

Figure 6. MCPA removal efficiencies M-GO/S, commercially available activated carbon (AC) (Adam Carbons Limited, Sri Lanka), and normal filtered sand

Conclusion

The study successfully developed an HPLC method tailored for analyzing MCPA at mg/L levels, which facilitated an in-depth investigation of MCPA adsorption onto M-GO/S. The optimized HPLC setup, utilizing a 50:50 mixture of acetonitrile and distilled water as the mobile phase, with a flow rate of 1.5 µL/min and a detection wavelength of 275 nm, provided precise and consistent analytical results. Isotherm studies indicated that both the Langmuir and Freundlich models fit well, likely due to the occurrence of multilayered adsorption followed by monolayer adsorption, as suggested by the similar R^2 values. The adsorption intensity (n) further highlighted the complexity of the MCPA adsorption process, pointing to intricate interactions between MCPA and the surface of M-GO/S. Kinetic studies revealed that the adsorption process is likely controlled by chemical adsorption, with significant electron sharing or transfer between the adsorbent and MCPA. The strong adsorption of MCPA, facilitated by hydrogen bonding and interactions between the hydroxyl groups of M-GO/S and the aromatic rings of MCPA, underscores the efficacy of the material. Given its exceptional adsorption capacity for various contaminants, including fluoride, and its proven ability to remove water turbidity and calcium from hard water, M-GO/S emerges as a highly promising candidate for water purification. Its superiority over GO, sand, and activated carbon lies in its ability to adsorb multiple contaminants simultaneously and its ease of recovery. Furthermore, the cost-effective bulk production of M-GO/S positions it as a viable option for real-world applications, warranting further investigation into its broader environmental benefits.

Acknowledgement

The authors wish to express their gratitude to the National Institute of Fundamental Studies in Kandy for providing the instruments necessary for this project.

Conflict of interest statement

Authors have no competing interests to declare.

References

Abo El-Maali, N., Nemr, A., Abd El–Wahab, M., & Moharram, A. (2018). Monitoring of removal of organochlorine/fluorine pesticides from water using graphene composites by gas chromatography/mass spectrometry. *Journal of Water Chemistry and Technology, 40*(4), 234–240. https://doi.org/10.3103/S1063455X18040094

Chu, S., Huang, W., Shen, F., Li, T., Li, S., Xu, W., Lv, C., Luo, Q., & Liu, J. (2020). Graphene oxide-based colorimetric detection of organophosphorus pesticides via a multi-enzyme cascade reaction. *Nanoscale, 12*(10), 5829–5833. https://doi.org/10.1039/C9NR10862A

El-Shamy, O. A. A., Nassar, I. M., & Ragab, A. A. (2023). Facile synthesis of graphene sand composite from asphalt as an effective adsorbent for chromium ions in aqueous media. *Polymer Bulletin, 80*(9), 9899–9911. https://doi.org/10.1007/s00289-022-04545-z

Faysal Hossain, M., Akther, N., & Zhou, Y. (2020). Recent advancements in graphene adsorbents for wastewater treatment: Current status and challenges. *Chinese Chemical Letters, 31*(10), 2525–2538. https://doi.org/10.1016/j.cclet.2020.05.011

Gao, W., Majumder, M., Alemany, L. B., Narayanan, T. N., Ibarra, M. A., Pradhan, B. K., & Ajayan, P. M. (2011). Engineered graphite oxide materials for application in water purification. *ACS Applied Materials & Interfaces, 3*(6), 1821–1826. https://doi.org/10.1021/am200300u

Garrido, E. M., Santos, M., Silva, P., Cagide, F., Garrido, J., & Borges, F. (2012). Host-guest complexes of phenoxy alkyl acid herbicides and cyclodextrins. MCPA and β-cyclodextrin. *Journal of Environmental Science and Health, Part B, 47*(9), 869–875. https://doi.org/10.1080/03601234.2012.693867

Hasanuddin, N. I., Dzulkifli, N. N., Sarijo, S. H., & Ghazali, S. A. I. S. M. (2020). Physicochemical characterization and controlled release formulation on intercalated 2-methyl-4-chlorophenoxy acetic acid-graphite oxide (MCPA-GO) nanocomposite. *Indonesian Journal of Chemistry, 20*(2), 299. https://doi.org/10.22146/ijc.40921

Imamoglu, M., & Tekir, O. (2008). Removal of copper (II) and lead (II) ions from aqueous solutions by adsorption on activated carbon from a new precursor hazelnut husks. *Desalination, 228*(1–3), 108–113. https://doi.org/10.1016/j.desal.2007.08.011

Jeppu, G. P., & Clement, T. P. (2012). A modified Langmuir-Freundlich isotherm model for simulating pH-dependent adsorption effects. *Journal of Contaminant Hydrology, 129–130*, 46–53. https://doi.org/10.1016/j.jconhyd.2011.12.001

Jia, F., Xiao, X., Nashalian, A., Shen, S., Yang, L., Han, Z., Qu, H., Wang, T., Ye, Z., Zhu, Z., Huang, L., Wang, Y., Tang, J., & Chen, J. (2022). Advances in graphene oxide membranes for water treatment. *Nano Research, 15*(7), 6636–6654. https://doi.org/10.1007/s12274-022-4273-y

Kumarasinghe, A. R., Perera, W. P. R. T., Bandara, J., Rukshagini, P., Jayarathe, L., Liyanage, J. A., Tennakone, R., Bandara, A., Chen, X., & Weerasooriya, R. (2021a). Multiple coated graphite oxide–sand composites for fluoride removal in water. *Journal of Environmental Chemical Engineering, 9*(2), 104962. https://doi.org/10.1016/j.jece.2020.104962

Kumarasinghe, A. R., Perera, W. P. R. T., Bandara, J., Rukshagini, P., Jayarathe, L., Liyanage, J. A., Tennakone, R., Bandara, A., Chen, X., & Weerasooriya, R. (2021b). Multiple coated graphite oxide–sand composites for fluoride removal in water. *Journal of Environmental Chemical Engineering, 9*(2), 104962. https://doi.org/10.1016/j.jece.2020.104962

Lazarević-Pašti, T., Anićijević, V., Baljozović, M., Anićijević, D. V., Gutić, S., Vasić, V., Skorodumova, N. V., & Pašti, I. A. (2018). The impact of the structure of graphene-based materials on the removal of organophosphorus pesticides from water. *Environmental Science: Nano, 5*(6), 1482–1494. https://doi.org/10.1039/C8EN00171E

Li, Y., Zhu, J., Li, S., Guo, Z., & Van Der Bruggen, B. (2020). Flexible aliphatic–aromatic polyamide thin film composite membrane for highly efficient organic solvent nanofiltration. *ACS Applied Materials & Interfaces, 12*(28), 31962–31974. https://doi.org/10.1021/acsami.0c07341

Lian, Q., Ahmad, Z. U., Gang, D. D., Zappi, M. E., Fortela, D. L. B., & Hernandez, R. (2020). The effects of carbon disulfide driven functionalization on graphene oxide for enhanced Pb(II) adsorption: Investigation of adsorption mechanism. *Chemosphere, 248*, 126078. https://doi.org/10.1016/j.chemosphere.2020.126078

Lian, Q., Islam, F., Ahmad, Z. U., Lei, X., Depan, D., Zappi, M., Gang, D. D., Holmes, W., & Yan, H. (2021). Enhanced adsorption of resorcinol onto phosphate functionalized graphene oxide synthesized via Arbuzov reaction: A proposed mechanism of hydrogen bonding and π-π interactions. *Chemosphere, 280*, 130730. https://doi.org/10.1016/j.chemosphere.2021.130730

Mahdavi-Shakib, A., Rich, L. C., Whittaker, T. N., & Chandler, B. D. (2021). Hydrogen adsorption at the Au/TiO_2 interface: Quantitative determination and spectroscopic signature of the reactive interface hydroxyl groups at the active site. *ACS Catalysis, 11*(24), 15194–15202. https://doi.org/10.1021/acscatal.1c04419

Mandeep, Gulati, A., & Kakkar, R. (2020a). Graphene-based adsorbents for water remediation by removal of organic pollutants: Theoretical and experimental insights. *Chemical Engineering Research and Design, 153*, 21–36. https://doi.org/10.1016/j.cherd.2019.10.013

Mandeep, Gulati, A., & Kakkar, R. (2020b). Graphene-based adsorbents for water remediation by removal of organic pollutants: Theoretical and experimental insights. *Chemical Engineering Research and Design, 153*, 21–36. https://doi.org/10.1016/j.cherd.2019.10.013

Moral, A., Caballo, C., Sicilia, M. D., & Rubio, S. (2012). Highly efficient microextraction of chlorophenoxy acid herbicides in natural waters using a decanoic acid-based nanostructured solvent prior to their quantitation by liquid chromatography–mass spectrometry. *Analytica Chimica Acta, 709*, 59–65. https://doi.org/10.1016/j.aca.2011.10.016

Nasiri, M., Ahmadzadeh, H., & Amiri, A. (2021). Organophosphorus pesticides extraction with polyvinyl alcohol coated magnetic graphene oxide particles and analysis by gas chromatography-mass spectrometry: Application to apple juice and environmental water. *Talanta, 227*, 122078. https://doi.org/10.1016/j.talanta.2020.122078

Osawa, E., Kitamura, K., & Yoshida, Z. (1967). Spectra and hydrogen bonding of diphenylcyclopropenone. *Journal of the American Chemical Society, 89*(15), 3814–3817. https://doi.org/10.1021/ja00991a023

Paramasivan, T., Sivarajasekar, N., Muthusaravanan, S., Subashini, R., Prakashmaran, J., Sivamani, S., & Ajmal Koya, P. (2019). Graphene family materials for the removal of pesticides from water. In M. Naushad (Ed.), *A new generation material graphene: Applications in water technology* (pp. 309–327). Springer. https://doi.org/10.1007/978-3-319-75484-0_13

Perera, W. P. R. T. (2023). Water hardness and health. In M. N. V. Prasad & M. Vithanage (Eds.), *Medical geology* (1st ed., pp. 129–141). Wiley. https://doi.org/10.1002/9781119867371.ch8

Suo, F., Xie, G., Zhang, J., Li, J., Li, C., Liu, X., Zhang, Y., Ma, Y., & Ji, M. (2018). A carbonised sieve-like corn straw cellulose–graphene oxide composite for organophosphorus pesticide removal. *RSC Advances, 8*(14), 7735–7743. https://doi.org/10.1039/C7RA12898C

Uddin, M. T., Islam, M. A., Mahmud, S., & Rukanuzzaman, M. (2009). Adsorptive removal of methylene blue by tea waste. *Journal of Hazardous Materials, 164*(1), 53–60. https://doi.org/10.1016/j.jhazmat.2008.07.131

Wang, M., Niu, Y., Zhou, J., Wen, H., Zhang, Z., Luo, D., Gao, D., Yang, J., Liang, D., & Li, Y. (2016). The dispersion and aggregation of graphene oxide in aqueous media. *Nanoscale, 8*(30), 14587–14592. https://doi.org/10.1039/C6NR03503E

Wu, F.-C., Tseng, R.-L., Huang, S.-C., & Juang, R.-S. (2009). Characteristics of pseudo-second-order kinetic model for liquid-phase adsorption: A mini-review. *Chemical Engineering Journal, 151*(1–3), 1–9. https://doi.org/10.1016/j.cej.2009.02.024

Yuqing, Y., Liangtong, Z., Li, Z., & Na, H. (2024). Evaluation of graphene oxide-coated sand adsorption on ammonium, lead and FA with molecular dynamic simulation and spectral induced polarization. *Environmental Earth Sciences, 83*(9), 282. https://doi.org/10.1007/s12665-024-11566-6

Zhu, D., Kwon, S., & Pignatello, J. J. (2005). Adsorption of single-ring organic compounds to wood charcoals prepared under different thermochemical conditions. *Environmental Science & Technology, 39*(11), 3990–3998. https://doi.org/10.1021/es050129e